Population Analysis of the Cingulum Bundle using the Tubular Surface Model for Schizophrenia Detection

Vandana Mohan[a] Ganesh Sundaramoorthi[b] Marek Kubicki[c] Douglas Terry[c] Allen Tannenbaum[a]

[a]School of Electrical and Computer Engineering, Georgia Institute of Technology, Atlanta, GA, USA
[b]Computer Science Department, University of California, Los Angeles, CA, USA
[c]Surgical Planning Laboratory, Brigham and Women's Hospital, Boston, MA, USA.

ABSTRACT

We propose a novel framework for population analysis of DW-MRI data using the Tubular Surface Model. We focus on the Cingulum Bundle (CB) - a major tract for the Limbic System and the main connection of the Cingulate Gyrus, which has been associated with several aspects of Schizophrenia symptomatology. The Tubular Surface Model represents a tubular surface as a center-line with an associated radius function. It provides a natural way to sample statistics along the length of the fiber bundle and reduces the registration of fiber bundle surfaces to that of 4D curves. We apply our framework to a population of 20 subjects (10 normal, 10 schizophrenic) and obtain excellent results with neural network based classification (90% sensitivity, 95% specificity) as well as unsupervised clustering (k-means). Further, we apply statistical analysis to the feature data and characterize the discrimination ability of local regions of the CB, as a step towards localizing CB regions most relevant to Schizophrenia.

1. INTRODUCTION

Schizophrenia involves a broad range of functional disturbances, including attention, memory, emotion, motivation, thought and language, social functioning, and mood regulation. A significant body of work [1–3] supports the speculation that functional abnormalities in Schizophrenia might be caused by disruptions of white matter (WM) connections. Also, several aspects of behavior associated with Cingulate Gyrus (CG) function such as attentional processing,memory, motivation and emotion, have been implicated in Schizophrenia making the study of the CG significant and since the proper functioning of the CG depends on its connections with other parts of the neuronal network, the study of WM interconnecting the CG and other parts of the human brain is very important. In this work, we focus on studying the main connection of the CG - the Cingulum Bundle (CB).

Diffusion-Weighted MRI (DWI) is an imaging modality extremely useful in the study and characterization of WM properties. It describes the diffusion of water molecules along multiple sampling directions at each voxel of the image. While diffusion can be treated as isotropic in Cerebro-Spinal Fluid (CSF) and to a certain extent in gray matter, along fiber tracts, it is highly anisotropic since the diffusion of intra- and extra- cellular fluid is inhibited at tract boundaries. This difference in anisotropy and diffusivity forms the basis of all approaches to tractography and fiber bundle segmentation. Clinical studies aimed at detection of Schizophrenia have typically focused on using statistics in a volumetric analysis framework, or along individual fiber tracts [4] (which requires co-registration of the multiple fiber tracts from different subjects). In this work, we compare statistics along the length of the fiber bundles which allows us to both look for local differences and also better address the classical DWI issues of noise and low resolution since we don't look along individual fibers.

1.1 The Cingulum Bundle and Schizophrenia

Several aspects of behavior associated with CG funtion such as attentional processing and emotion, are implicated in Schizophrenia making it significant to study the CG. CG abnormalities include bilateral CG volume and density reduction in voxel-based morphometric studies . Volume deficits in structural MRI studies have also been (albeit inconsistently) associated with hallucinations, reduced executive functions, psychomotor poverty and negative symptoms. The proper functioning of the CG depends on connections with other parts of the neuronal network,

Medical Imaging 2010: Computer-Aided Diagnosis, edited by Nico Karssemeijer, Ronald M. Summers,
Proc. of SPIE Vol. 7624, 762429 · © 2010 SPIE · CCC code: 1605-7422/10/$18 · doi: 10.1117/12.844297

rather than simply its structure alone. A significant body of work [1–3] supports the speculation that functional abnormalities in Schizophrenia might be caused by disruptions of WM connections. The CG itself connects to other brain regions via two major tracts - the Cingulum Bundle (CB) and the Uncinate Fasciculus (UF). Several symptoms of schizophrenia, including paranoia, hallucinations, and delusions, have been linked to a disruption in frontal and anterior temporal regions traveling through the UF and CB. Moreover, these tracts are involved in deficits in executive attention, memory encoding, declarative-episodic verbal memory, as well as verbal and visual memory. The study of these two fiber bundles is therefore key to understanding Schizophrenia and in this work, we focus on one of these bundles - the Cingulum Bundle (CB).

2. PRIOR WORK

Diffusion Tensor Imaging (DTI) has become the modality of choice for studying WM properties. Many approaches exist in the literature for DTI processing towards Schizophrenia discrimination motivated by the increasing evidence in the literature for WM abnormalities in Schizophrenia [1,5,6] supporting the hypothesis of Friston et al [7] regarding disordered connectivity between brain regions in Schizophrenia. One set of methods looks into finding WM deficits associated directly with the disease, by studying Fractional Anisotropy (FA) and Apparent Diffusion Coefficient (ADC). Caprihan et al [8] used a voxel-based strategy and applied Discriminatory PCA (DPCA) to Fractional Anisotropy (FA) measurements to discriminate between schizophrenic and normal controls. Goodlett et al [9] performed statistical comparison of fiber bundle diffusion properties between populations of DTI images, by using permutation testing based on the Hotelling T^2 statistic (for studying neurodevelopment). Park et al [10] studied hemispherical WM asymmetries by a statistical comparison of normalized FA images and the flipped images (of FA), and found evidence of asymmetry in anisotropy patterns between healthy and schizophrenic subjects. A second set of methods looks into studying the correlation of WM properties with specific symptoms and symptom groups, since it is observed that symptom profiles can vary significantly between subjects in Schizophrenia. Skelly el al [11] compared FA between schizophrenic and normal controls and performed a voxel-wise correlational analysis with the subjects' Positive and Negative Symptoms Scales (PANSS). Fujiwara et al [12] studied abnormalities in the CB (anterior and posterior) and their correlation with the psychopathology of schizophrenia, via a correlation analysis of FA with PANSS scores.

To our knowledge, this is the first group study that uses DW-MRI data directly (for segmentation) without imposing the elliptical constraint associated with tensor estimation. Also, by the very nature of the model used for the CB, we are better equipped to evaluate its different spatial regions for abnormalities caused by Schizophrenia. The work of Fujiwara et al [12] and Wang et al [13] are steps in the direction of determining local differences in Schizophrenia. Both these studies focused on dividing the CB into 2 regions - anterior and posterior - and this is the subdivision that we consider in this work. However our framework allows for subdividing the CB into as many regions for analysis as desired.

3. TUBULAR SURFACE MODEL

In this section, we discuss the Tubular Surface Model of Mohan et al [14] and motivate its application to population studies on neural fiber bundles.

3.1 Reviewing the model

In the work of Mohan et al,[14] a tubular surface is modeled as being determined by a center line that is an open curve in $\mathbb{R}^3$, and a radius function defined at every point of this center-line. Given an open curve $c : [0,1] \rightarrow \mathbb{R}^3$, the center line, and a function $r : [0,1] \rightarrow \mathbb{R}^+$, the radius function, the tubular surface , $S : \mathbb{S}^1 \times [0,1] \rightarrow \mathbb{R}^3$ ($\mathbb{S}^1$ is $[0, 2\pi]$ with endpoints identified) is defined as follows:

$$S(\theta, u) = c(u) + r(u)[n_1(u)\cos\theta + n_2(u)\sin\theta] \tag{1}$$

where $n_1, n_2 : [0,1] \rightarrow \mathbb{R}^3$ are normals to the curve c defined to be orthonormal, smooth, and such that the dot products $c'(u) \cdot n_i(u)$ vanish, $u \in [0,1]$ is the arc-length parameterization and $theta \in [0, 2\Pi]$ is the angle at a given point u of the center-line over the cross-section of the surface. Figure 1 show an illustration of a tubular surface.

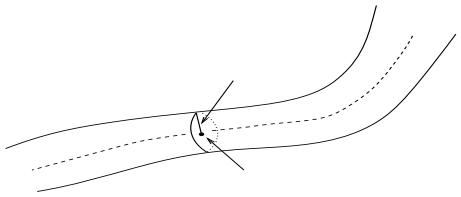

Figure 1: Illustration of Tubular Surface model

The tubular surface is represented as a collection of circles each lying in the plane perpendicular to the center line. It is worth noting that the surface in (1) may now be identified with a 4D space curve, $\tilde{c} : [0, 1] \rightarrow \mathbb{R}^4$:

$$\tilde{c}(u) = (c(u), r(u))^T. \tag{2}$$

3.2 Application of the model in population studies

The Tubular Surface Model affords a natural way to compare fiber bundles since the parametric representation of the surface in 3D as a curve in 4D allows the sampling of features along the length of the tubular surface. Further, the problem of registering surfaces is reduced to one of registering curves. In order to perform population studies using the model, we need co-registration of the feature vectors formed from the tubular surfaces. Towards this objective, we define three operations on the tube in our model: average tube, average of functions defined on/around the the boundary of the tube, and the distance between a (sample) tube and the average tube.

We define an average tube as represented by a center-line, $\hat{c}$ and $\hat{r}$, with $\hat{c}$ as:

$$\hat{c}, \{\phi_i\}_{i=1}^N = \underset{\hat{c}, \{\phi_i\}_{i=1}^N}{\arg\min} \sum_{i=1}^{N} \int_0^1 |K_{\hat{c}}(\hat{s}(\phi_i(u))) - K_{c_i}(u)|^2 \, \mathrm{d}u; \tag{3}$$

we have the following constraint on reparameterizations $\phi_i : [0, 1] \rightarrow [0, 1]$:

$$\phi_i(0) = 0, \phi_i(1) = 1, \text{ and } \phi_i' > 0 \tag{4}$$

that is, ϕ_i are monotone diffeomorphisms. Above, $\hat{s}$ is the arclength function of $\hat{c}$. In (3), $K_c : [0, 1] \rightarrow \mathbb{R}^n$ ($n \geq 1$) is a pointwise "feature" vector of the curve c. In this paper, the CB representations were aligned lengthwise under the assumption that the different regions of the CB occupied the same intervals of length along the CB in all subjects. (Alternate criteria for registration are being explored in future work.)

From the correspondence functions ϕ_i, we define an average radius function $\hat{r}$ as:

$$\hat{r}(\hat{s}) = \frac{1}{N} \sum_{i=1}^{N} r_i \circ \phi_i^{-1}(\hat{s}) \tag{5}$$

We also use the correspondence functions, ϕ_i, to pullback functions from the tubes represented by (c_i, r_i) to the average tubular structure. Let $F : \mathbb{R}^3 XR \rightarrow \mathbb{R}^M$ ($M \geq 1$) be some function defined on $\mathbb{R}^3$ (and in particular inside the tube). We consider the function as being defined along the curve in 4D and we define the average function $\hat{F}$ as:

$$\hat{F}(\hat{c}, \hat{r}) = \frac{1}{N} \sum_{i=1}^{N} F_i(\hat{c} \circ \phi_i^{-1}(\hat{s}), \hat{r} \circ \phi_i^{-1}(\hat{s})) \tag{6}$$

We also define the corresponding standard deviation function as:

$$\sigma_F^2(\hat{c}, \hat{r}) = \frac{1}{N} \sum_{i=1}^{N} \|F_i(\hat{c} \circ \phi_i^{-1}(\hat{s}), \hat{r} \circ \phi_i^{-1}(\hat{s})) - \hat{F}(\hat{c}, \hat{r})\|^2 \tag{7}$$

Finally, to find the distance between the average $\hat{F}$ and a new test function F_t defined on a tubular surface (c_t,r_t) , we find a correspondence as:

$$\phi_t = \arg\min_{\phi_t} \int_0^1 |K_{\hat{c}}(\hat{s}(\phi_t(u))) - K_{c_t}(u)|^2 \, \mathrm{d}u, \tag{8}$$

and then we can define a distance between functions:

$$d(\{\hat{F}, \hat{c}, \hat{r}\}, \{F_t, c_t, r_t\}) = \int_0^1 \|\hat{F}(\hat{c}(\hat{s}), \hat{r}(\hat{s})) - F_t(c_t \circ \phi_t^{-1}(\hat{s}), r_t \circ \phi_t^{-1}(\hat{s}))\|^2 \, \mathrm{d}\hat{s} \tag{9}$$

4. POPULATION ANALYSIS FRAMEWORK

In this work, we use the Tubular Surface Model to segment the Cingulum Bundle (CB) from the DWI images. We then build feature vectors by sampling features along the length of the CB. In this section, we discuss the selection of features for classification and the techniques employed for statistical analysis on these features.

4.1 Feature extraction

In this work, we use the following features to describe the CB: mean curvature, geometric curvature, normalized cross-sectional area, center-shifted coordinates (as defined in [15]), Fractional Anisotropy (FA) and Mean Diffusion (MD). FA and MD characterize the WM properties while mean curvature, geometric curvature and the center-shifted coordinates encode shape information. The normalized cross-sectional area incorporates the thickness of the WM connections. Note that this usage of a combination of features is a significant improvement over prior approaches (E.g.[4,8]) which fundamentally employed only WM properties such as FA in a volumetric analysis framework. Further, while we sample along the center-line, the features are in fact extracted over the entire fiber bundle volume and hence this choice of sampling while facilitating registration, does not reduce the statistical power of our results. Finally, besides using a combination of these features for classification, we also compare their discrimination ability.

4.2 Statistical Analysis

The classification step in this work has the twin goals of robust discrimination between schizophrenic and normal controls, and also of characterizing the discrimination ability of the different spatial regions of the CB. In this work, we perform four sets of statistical analyses - t-statistical tests, supervised classification using neural networks, unsupervised classification (clustering) using the k-means algorithm and Potts model based clustering and finally correlational analysis of the extracted features with the symptom scores (PANSS) versus simply the diagnosis.

The t-statistical tests are aimed fundamentally at characterizing the spatial variation in discrimination ability. Since we build multiple features at each sample point along the center-line of the tubular surface, we estimate t-statistics with respect to all these features, and subsequently scale each category of features and sum the t-statistics for all features at each point, to get a comprehensive estimate of the t-statistic in a spatial sense. They also allow us to compare the discrimination ability of different categories of features such as shape information versus FA. The second technique is supervised classification using an Artificial Neural Network. In this work, we use the Neural Network toolbox of MATLAB[16] to build and train a simple feed-forward Backpropagation network with 1 hidden layer (having 5 neurons). The classification results obtained using the same are provide under the results section 5. The third technique is unsupervised classification (clustering). The goal for applying clustering techniques in the context of this work is to detect natural clusters in the feature data extracted, and validate the results from the surpervised classification to ensure robustness given the limited size of the population used for testing (details in Section 5.1). In this work, we perform clustering using the K-means algorithm [17,18] with a target of 2 clusters. Finally, in correlational analysis, we look at the correlation coefficients for the extracted features along the length of the bundle, with respect to the positive and negative symptom scores (the PANSS scale). This allows us to interpret regions with higher correlation with the symptom scores as being significant in Schizophrenia.

(a) Mean Curvature (b) Geometric Curvature (c) Center-shifted coordinates

(d) FA (e) Mean Diffusion (f) Crosssectional area

Figure 2: Visualization of t-statistics (by feature) on Cingulum Bundle surface (discrimination ability increases from green to red regions)

Table 1: Local peaks of discrimination ability

CB region	T-value (Left, local maximum)	T-value (Right, local maximum)
Anterior	4.643	4.372
Posterior	5.529	5.886

5. RESULTS & DISCUSSION

5.1 Data

The DWI imagery used in this work was acquired on a 3T magnet using an echo planar imaging (EPI) DTI Tensor sequence with a double echo option to reduce eddy-current related distortions (Heid 2000; Alexander 1997). The data was acquired in 51 directions with b=900, 8 baseline scans with b=0. Scan parameters are: TR 17000 ms, TE 78 ms, FOV 24 cm, 144x144 encoding steps, 1.7 mm slice thickness. 85 axial slices were acquired parallel to the AC-PC line covering the whole brain. The population analysed comprised 20 male subjects - 10 normal controls and 10 schizophrenic - spanning the age group of 21-55 years (mean of ~ 43 years).

5.2 Experiments

In this work, we use the framework of Mohan et al[14] to segment the Cingulum Bundle (CB) from the 20 data sets in the population under study. We extract feature vectors as described in Section 4.1 and register the same using Equations 3,5,6 and 7. Figure 2 shows the t-statistics visualized over the fiber bundle surface for both the right and

Table 2: Classification performance

Classification method	Type	Side	Classification Accuracy	Sensitivity (L)	Specifivity (R)
Neural networks	Supervised	Left	100%	90%	96%
Neural networks	Supervised	Right	100%	90%	94%
K-means	Unsupervised	Left	78%	83%	71%
K-means	Unsupervised	Right	75%	80%	69%

Table 3: Correlational Analysis (with PANSS positive symptom scores)

Feature	Mean correlation coefficient (L)	Mean correlation coefficient (R)	Maximum correlation coefficient (L)	Maximum correlation coefficient (R)	Region with maximum correlation coefficient (L)	Region with maximum correlation coefficient (R)	Significant Region (combining left and right sides)
Mean Curvature	0.8077	0.8078	0.9079	0.9062	RAC	RAC	RAC
Geometric Curvature	0.7261	0.7230	0.9450	0.8794	RAC	RAC	RAC
Center-shifted coordinates	0.4529	0.4778	0.6692	0.9146	RAC	RAC	RAC
Fractional Anisotropy	0.7920	0.7957	0.9412	0.9545	PC	PC	PC
Mean Diffusion	0.8100	0.8096	0.9094	0.9139	PC	PC	PC
Cross-sectional area	0.7094	0.6506	0.8957	0.8308	RAC	CAC	CAC
Bucket-of-features	-	-	-	-	RAC	RAC	RAC

RAC - Rostral anterior cingulate; CAC - Caudal anterior cingulate; PC - Posterior cingulate

Table 4: Correlational Analysis (with PANSS negative symptom scores)

Feature	Mean correlation coefficient (L)	Mean correlation coefficient (R)	Maximum correlation coefficient (L)	Maximum correlation coefficient (R)	Region with maximum correlation coefficient (L)	Region with maximum correlation coefficient (R)	Significant Region (combining left and right sides)
Mean Curvature	0.7335	0.7348	0.8415	0.8440	RAC	RAC	RAC
Geometric Curvature	0.6589	0.6569	0.8637	0.8276	RAC	RAC	RAC
Center-shifted coordinates	0.3855	0.3538	0.6690	0.5826	RAC	RAC	RAC
Fractional Anisotropy	0.7157	0.7195	0.8917	0.8674	PC	PC	PC
Mean Diffusion	0.7362	0.7355	0.8519	0.8494	RAC	RAC	RAC
Cross-sectional area	0.6862	0.6235	0.8847	0.8141	CAC	CAC	CAC
Bucket-of-features	-	-	-	-	RAC	RAC	RAC

RAC - Rostral anterior cingulate; CAC - Caudal anterior cingulate; PC - Posterior cingulate

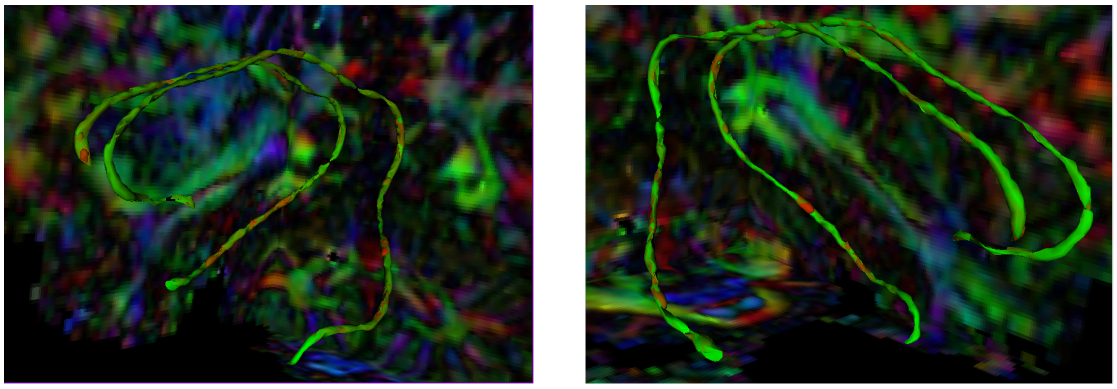

Figure 3: Visualization of t-statistics (consolidated) on Cingulum Bundle surface, overlaid on DTI data of one subject (discrimination ability increases from green to red regions)

left CB, separated by feature. We can see a correlation in the spatial patterns evidenced by the FA, Mean Diffusion and cross-sectional area. Interestingly, while the center-shited coordinates highlight multiple regions of the CB as being significant, we do see that the spatial patterns shown by the geometric curvature correlate with those of the diffusion-related features. Figure 3 shows us a consolidated view of the spatial t-statistics (with all features equally weighted). We can see clearly that this visualization highlights regions that are most significant in Schizophrenia classification (in red) allowing us to probe for anatomical explanations of the relevance of these specific regions. Note that the model allows us to subdivide the CB into as many subregions as desired for study, however in this work, we have divided it simply into anterior and posterior regions as a proof-of-concept and we include these statistics in Table 1. We are currently looking into using Region Of Interest (ROI) maps for regions along the CB as indicated by clinical experts. By using these ROIs to register the different CBs, we will be able to quantify the discrimination ability of anatomically meaningful regions. The results of these experiments on classification are summarized in Table 2. We obtained excellent classification with Neural Networks. Given the size of the population under study, to address the potential concern of over-fitting, we also conducted unsupervized clustering. We obtained promising results on the feature space discussed in this work, and are pursuing both the use of a larger population for increased robustness of the results, as well as additional features to descibe the CB so as to enhance natural clusters. Note that the sensitivity and specificity reported in Table 2 were estimated using a Leave-two-out validation strategy for the Neural Network. To estimate comparable metrics for the K-means algorithm, we "classified" two data sets at a time using the clusters obtained for the remaining 18 data sets.

Finally, we performed correlational analysis on the extracted features towards understanding their relationship to the symptom scores (versus simply the diagnosis) and the results of this analysis are summarized in Tables 3 and 4. We use here the PANSS scores of the 10 schizoprenic cases in the data set under study and the CB is divided into 6 regions (ordered from anterior to posterior) corresponding to gray matter regions identified by expert marking: Rostral anterior cingulate, Caudal anterior cingulate, Posterior cingulate, Isthmus cingulate, Parahippocampal gyrus and Entorhinal cortex. The correlational analysis reveals some interesting results in that the Rostral anterior cingulate (RAC) is identified most consistently as the most significant region along the CB fiber bundle volume with respect to involvement in Schizophrenia (by way of correlation with PANSS scores as represented by the correlation coefficient). The identification of the anterior region as being significant in Schizophrenia is consistent with the observations made in prior work[12, 13, 19] and our method allows us to further localize the region of interest to the RAC. For a more detailed discussion on PANSS scores, the interested reader is referred to the work of Kay et al. [20]

6. CONCLUSION

In this work, we propose a novel framework for population analysis of neural fiber bundles that employs the Tubular Surface Model of Mohan et al,[14] and performs the dual tasks of statistical analysis and visualization. We test this framework sucessfully on the Cingulum Bundle from a population of 20 data sets towards the detection of

Schizophrenia. Using t-statistical tests and correlation analysis, we demonstrate how the framework naturally characterizes the discrimination ability of different regions of the Cingulum Bundle in Schizophrenia and helps provide insight into the involvement of different regions in the disorder. We also obtain excellent classification using Neural Networks, and are able to verify natural clusters in the feature data by use of the K-means algorithm.

In future work, we plan to apply our framework to a larger population towards addressing potential concerns of over-fitting in the population used in this study. We are also exploring more features for decribing the CB including higher order shape information, towards improving the natural clustering.

REFERENCES

[1] Davis, K., Stewart, D., Friedman, J., Buchsbaum, M., Harvey, P., Hof, P., Buxbaum, J., and Haroutunian, V., "White Matter Changes in Schizophrenia Evidence for Myelin-Related Dysfunction," (2003).

[2] Hakak, Y., Walker, J., Li, C., Wong, W., Davis, K., Buxbaum, J., Haroutunian, V., and Fienberg, A., "Genome-wide expression analysis reveals dysregulation of myelination-related genes in chronic schizophrenia," *Proceedings of the National Academy of Sciences* **98**(8), 4746 (2001).

[3] Benes, F., "Relationship of cingulate cortex to schizophrenia and other psychiatric disorders," *Neurobiology of Cingulate Cortex and Limbic Thalamus: A Comprehensive Handbook. Boston: Birkh äuser* , 581–605 (1993).

[4] Corouge, I., Fletcher, P., Joshi, S., Gouttard, S., and Gerig, G., "Fiber tract-oriented statistics for quantitative diffusion tensor MRI analysis," *Medical Image Analysis* **10**(5), 786–798 (2006).

[5] Takase, K., Tamagaki, C., Okugawa, G., Nobuhara, K., Minami, T., Sugimoto, T., Sawada, S., and Kinoshita, T., "Reduced white matter volume of the caudate nucleus in patients with schizophrenia," *Neuropsychobiology* **50**(4), 296–300 (2004).

[6] Zai, G., King, N., Wigg, K., Couto, J., Wong, G., Honer, W., Barr, C., and Kennedy, J., "Genetic study of the myelin oligodendrocyte glycoprotein (MOG) gene in schizophrenia," *Genes, Brain & Behavior* **4**(1), 2–9 (2005).

[7] Friston, K., "The disconnection hypothesis," *Schizophrenia Research* **30**(2), 115–125 (1998).

[8] Caprihan, A., Pearlson, G., and Calhoun, V., "Application of principal component analysis to distinguish patients with schizophrenia from healthy controls based on fractional anisotropy measurements," *Neuroimage* **42**(2), 675–682 (2008).

[9] Goodlett, C., Fletcher, P., Gilmore, J., and Gerig, G., "Group analysis of DTI fiber tract statistics with application to neurodevelopment," *Neuroimage* (2008).

[10] Park, H., Westin, C., Kubicki, M., Maier, S., Niznikiewicz, M., Baer, A., Frumin, M., Kikinis, R., Jolesz, F., McCarley, R., et al., "White matter hemisphere asymmetries in healthy subjects and in schizophrenia: a diffusion tensor MRI study," *Neuroimage* **23**(1), 213–223 (2004).

[11] Skelly, L., Calhoun, V., Meda, S., Kim, J., Mathalon, D., and Pearlson, G., "Diffusion tensor imaging in schizophrenia: Relationship to symptoms," *Schizophrenia Research* (2008).

[12] Fujiwara, H., Namiki, C., Hirao, K., Miyata, J., Shimizu, M., Fukuyama, H., Sawamoto, N., Hayashi, T., and Murai, T., "Anterior and posterior cingulum abnormalities and their association with psychopathology in schizophrenia: A diffusion tensor imaging study," *Schizophrenia Research* **95**(1-3), 215–222 (2007).

[13] Wang, F., Sun, Z., Cui, L., Du, X., Wang, X., Zhang, H., Cong, Z., Hong, N., and Zhang, D., "Anterior cingulum abnormalities in male patients with schizophrenia determined through diffusion tensor imaging," (2004).

[14] Mohan, V., Sundaramoorthi, G., Melonakos, J., Niethammer, M., Kubicki, M., and Tannenbaum, A., "Tubular Surface Evolution for Segmentation of the Cingulum Bundle From DW-MRI," *MFCA08* , 150.

[15] Liang, X., Zhuang, Q., Cao, N., and Zhang, J., "Shape Modeling and Clustering of White Matter Fiber Tracts Using Fourier Descriptors," in [*IEEE Symposium on Computational Intelligence in Bioinformatics and Computational Biology, 2009. CIBCB'09*], 292–297 (2009).

[16] Demuth, H. and Beale, M., [*Neural Network Toolbox: for use with MATLAB*], The Math Works (2001).

[17] Kanungo, T., Mount, D., Netanyahu, N., Piatko, C., Silverman, R., and Wu, A., "An Efficient k-Means Clustering Algorithm: Analysis and Implementation," *IEEE Transactions on Pattern Analysis and Machine Intelligence* , 881–892 (2002).

[18] Hartigan, J. and Wong, M., "A K-means clustering algorithm," *JR Stat. Soc. Ser. C-Appl. Stat* **28**, 100–108 (1979).

[19] Baiano, M., David, A., Versace, A., Churchill, R., Balestrieri, M., and Brambilla, P., "Anterior cingulate volumes in schizophrenia: a systematic review and a meta-analysis of MRI studies," *Schizophrenia research* **93**(1-3), 1–12 (2007).

[20] Kay, S., Flszbein, A., and Opfer, L., "The positive and negative syndrome scale (PANSS) for schizophrenia," *Schizophrenia bulletin* **13**, 261–276 (1987).